Journal of the European Ceramic Society 15 (1995) 1185–1192

0955-2219(95)00102-6
0955-2219/95/$9.50

Mechanical Property Characterization of a 9 mol% Ce–TZP Ceramic Material — I. Flexural Response

G. A. Gogotsi,[a] V. P. Zavada[a] & M. V. Swain[b]

[a]Institute for Problems of Strength, Ukranian Academy of Sciences, 252014 Kiev, Ukraine
[b]Department of Mechanical and Mechatronic Engineering, The University of Sydney, NSW 2006, Australia

(Received 5 August 1994; revised version received 13 March 1995; accepted 31 May 1995)

Abstract

Investigations were carried out on four tetragonal zirconia polycrystalline (TZP) ceramics of differing grain size containing 9 mol% CeO_2. Precision flexural tests on these materials were conducted to determine the elastic modulus, the non-linear deflection and the associated acoustic emission during such testing. The deformation was characterized in terms of the number and size of the transformation bands that developed during the non-linear response. The finest grained material initially exhibited permanent set without the presence of such bands, whereas all the coarser grained materials showed a linear relationship between the summation of the band widths and the residual deflection. The acoustic emission and plastic strain behaviour are discussed in terms of the number and size of the stress induced phase transformation bands.

1 Introduction

The development of tough ductile ceramics has been the long cherished dream of many materials engineers. Recently this situation has to some extent been realised with the development of Ce–tetragonal zirconia polycrystalline (TZP) materials which behave almost like mild-steel as shown initially by Tsukuma and Shimada[1] and subsequently verified by numerous authors.[2–6] The main emphasis of such papers has been to rationalize the basis of the non-linear response and the development of bands where the tetragonal grains had transformed to monoclinic zirconia without any associated cracking.

Ce–TZP materials are somewhat unique amongst the zirconia phase transformable materials in that the tetragonal (t) to monoclinic (m) transformation exhibits burst or autocatalytic behaviour. Previous studies by Reyes-Morel and Chen,[4] and Becher and Swain[7] have investigated this behaviour and shown that a strong grain size effect exists and influences the burst temperature M_B for the t → m transformation. The latter authors have also provided a simple thermodynamic explanation of this size effect, relating it to a critical nuclei size and degree of undercooling or applied stress to initiate the transformation.

In this paper a more critical appraisal is given of the force–displacement response of the Ce–TZP materials tested in four point flexure. In particular the non-linear response is characterised in terms of the acoustic emission that develops and the size and number of the transformation bands. In a previous paper the authors[8] also investigated acoustic emission activity during the flexure testing of Mg–PSZ ceramics. However, that study did not enable an unambiguous interpretation of the acoustic emission (AE) data, that is, whether it was generated by stress induced phase-transformation or microcracking of the coarse grained microstructure of that material.

2 Materials

The investigations were carried out on Ce–TZP ceramics containing 9 mol% CeO_2. These materials were sintered at temperatures from 1400 to 1550°C in air for 1 h and their fabrication has been described by Grathwohl and Liu.[2] The designation, sintering temperature, mean grain size and relative density are listed in Table 1.

Specimens in the form of rectangular bars 2 × 2·8 × 48 mm were cut from a large sintered plate and polished on two adjacent sides prior to flexure testing. Four point bending tests were conducted on a precision rig described elsewhere[9] with inner and outer supports of 20 and 40 mm at a crosshead speed of 0·5 mm/min. The specimen deflection and accumulated acoustic emission counts were measured during the test using the same procedure as described in Ref. 8.

Table 1. Designation and properties of investigated ceramics

Designation	*Temperature of sintering (°C)*	*Mean grain size (μm)*	*Relative density (%)*
Ce–TZP-I	1400	1·14	94
Ce–TZP-II	1450	1·62	97
Ce–TZP-III	1500	2·22	98
Ce–TZP-IV	1550	3·00	97

3 Results and Discussion

3.1 Force–displacement curves

3.1.1 Monotonic loading

Typical force–displacement (P–δ) curves and associated acoustic emission counts (P–N_Σ) of the four ceramics are shown in Fig. 1(a–d), and the results are summarized in Table 2. The brittleness measure has been discussed in detail elsewhere by Gogotsi[9] and is the ratio of the elastic to the total energy under the force–displacement curve at the onset of fracture. It is clear from the data in Table 2 that the materials differ insignificantly in terms of their density, elastic modulus and ultrasonic velocity. The force–displacement curves are similar to those reported by Grathwohl and Liu[2] in that there is initially a linear response from which the 'static' estimate of the elastic modulus was calculated.

Beyond the linear response region of the P–δ curves the materials exhibit inelastic behaviour that may be approximated by a straight line whose slope decreases with increasing grain size of the Ce–TZP material as shown schematically in Fig. 2(a). The critical load at the onset of inelastic behaviour P_{el} and for failure P_m for each of the ceramics is shown in Fig. 2(b). The maximum deflection δ_m and residual deflection δ_r (maximum deflection less elastic recovery) are shown in Fig. 2(c). The residual or plastic deflection, δ_r, is almost independent of the grain size of the material.

The materials exhibit significant differences in the form of the inelastic portion of the P–δ deformation. The Ce–TZP-1 material exhibits a very smooth curve with the onset of nonlinear behaviour only being determined by the almost imperceptible change in slope. This behaviour is similar to that observed with Mg–PSZ (TS grade) material. Whereas the materials CE–TZP-II to Ce–TZP-IV are characterized by very jerky behaviour with the magnitudes of the intermittent

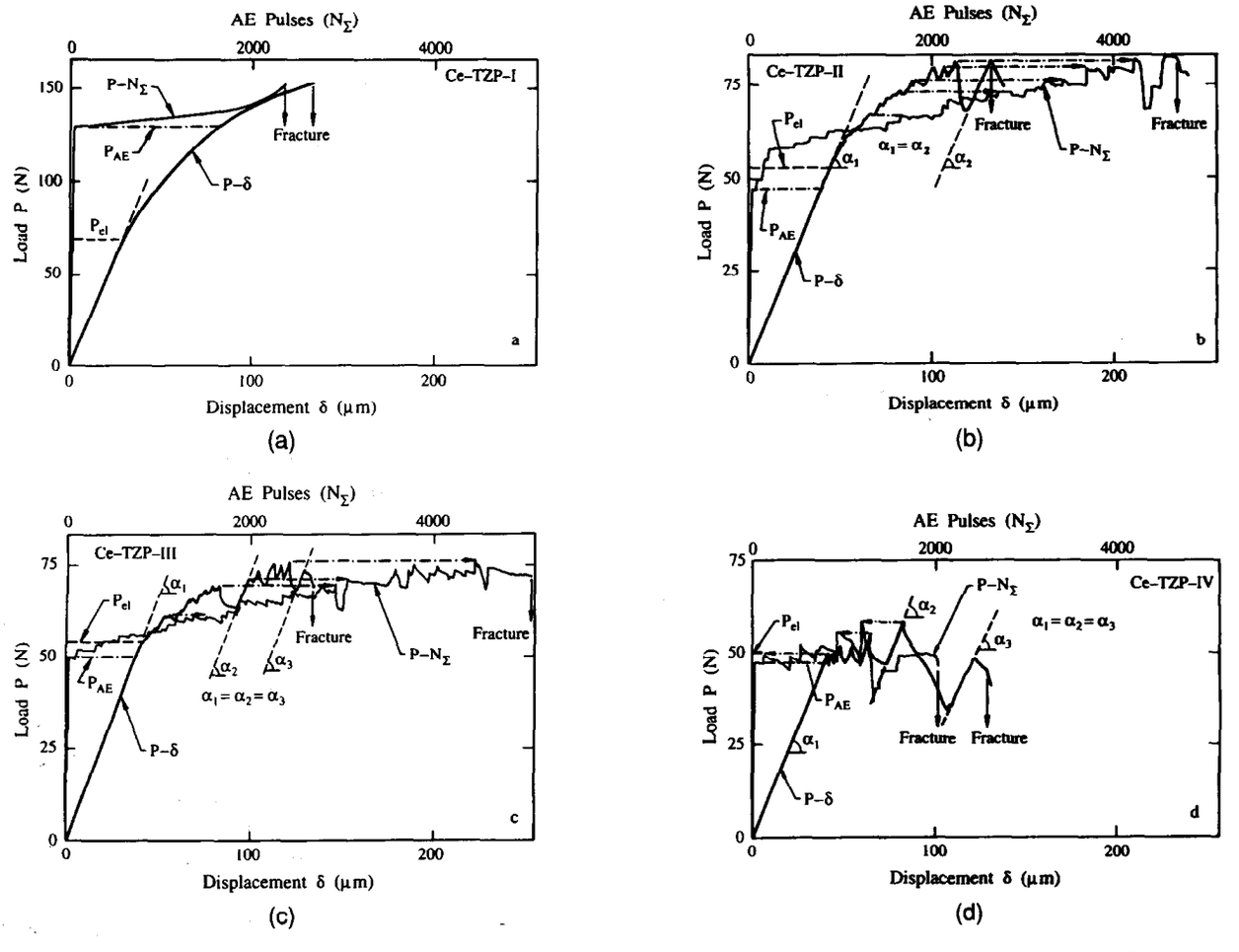

Fig. 1. Load–displacement (P–δ) and load–accumulated acoustic emission events (P–$N\epsilon$) for the four Ce–TZP materials. (a) Ce–TZP-I; (b) Ce–TZP-II; (c) Ce–TZP-III; and (d) Ce–TZP-IV.

Table 2. Physical and mechanical characteristics of Ce–TZP ceramics[a]

Ceramics	*Density* (g/cm^3)	*Ultrasound velocity* (*m/s*)	*MOR* (*MPa*)	*Ultimate strain* (10^{-4}*m/m*)	*Elasticity modulus* (*GPa*)		χ
					Dynamic	*Static*	
Ce–TZP-I	5·68	5459	451	47·3	175	169	0·34
Ce–TZP-II	6·00	5466	239	23·9	179	180	0·31
Ce–TZP-III	6·07	5465	223	23·5	181	175	0·15
Ce–TZP-IV	6·01	5411	177	28·7	176	175	0·15

[a]The crosshead speed is 0·5 mm/min.

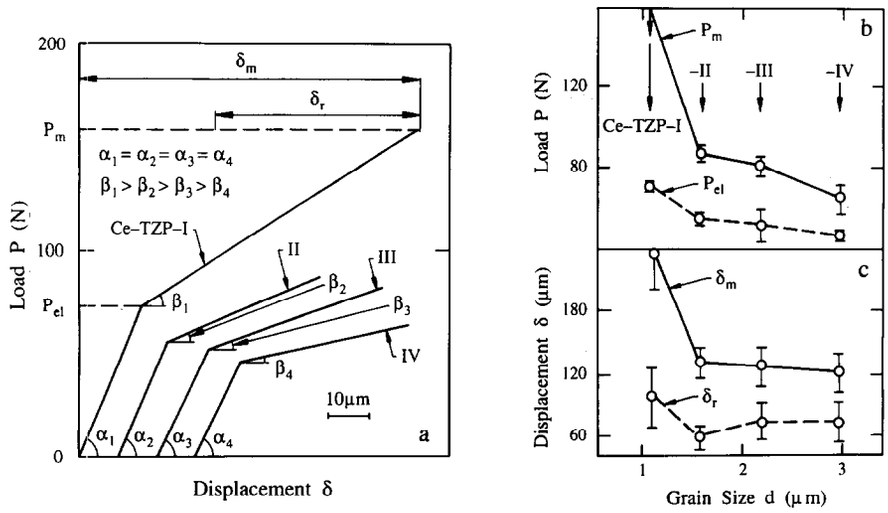

Fig. 2. (a) Schematic bi-linear approximation of the load–displacement diagrams for the various Ce–TZP materials; (b) comparison of the elastic limit load and maximum load; (c) the maximum and residual strain as a function of grain size.

load drops increasing with material grain size. These peculiarities of the P–δ response during monotonic loading appeared as part of the continuous load–deflection curves, and alternated with sharp load drops accompanied by an increase in deflection. It should also be noted that similar drops in load (but developing more slowly) were also occasionally observed for periods of up to a few minutes after the testing machine-crosshead had been stopped at maximum load. Thus although a time factor of loading can not be ruled out, nevertheless the shape of the P–δ curves did not essentially differ at crosshead speeds of 0·5 and 0·005 mm/min. Unfortunately, the limited number of samples did not enable this time dependent effect to be investigated in detail.

The nature of the load drops during continuous load–deformation curves should not be associated with the nucleation and growth of cracks in the specimen. Crack initiation or growth would lead to a change of the specimen compliance, $c = \tan^{-1}\alpha_1$ (Fig. 1(b, c or d)), by the value $\Delta c = \tan^{-1}\alpha_1 - \tan^{-1}\alpha_2$. Such a change in compliance should be related to a decrease in load ΔP_i by the relationship

$$\frac{\Delta c_i}{c_o} \simeq \frac{\Delta P_i}{P}.$$

This expression is also valid for the total change of specimen compliance Δc_i, which should be related to the sum of the successive load drops by the total value $\Sigma \Delta P_i$, i.e.

$$\frac{\Delta c_i}{c} \simeq \frac{\Sigma \Delta P_i}{P}.$$

The right-hand part of the above expression for samples Ce–TZP-III and -IV reaches 10–20%, such a change of compliance would have been readily measured on the reloading portion of the monotonic load–deflection curve after a few such load drops. However, the slope of these curves within the limit of experimental error (2–3%) showed undetectable change throughout the course of loading. In addition, the anticipated crack depth associated with such a load drop would have been readily visible, and in the range 0·6–1·0 mm.

Analysis of the acoustic emission data is of particular interest. This data which must be considered as only comparative because of the difficulty of attachment of the AE detector to such a small bar. It is for this reason that the total AE count to fracture was characterized by considerable scatter from specimen to specimen, which did not allow for example one to relate N_Σ values to

the grain size of the ceramics. However, the results consistently showed that for sample II, III and IV the onset of AE counts corresponds to the onset of nonlinearity of the P–δ curve, whereas for the Ce–TZP-I material the AE began only after considerable non-linearity. Also, one can clearly observe a correlation between AE outbursts and load drops (in Fig. 1(b–d) such correlations are connected by means of dashed horizontal lines). In contrast to this, very few AE events were detected during the continuous portions of the load–deflection curve.

3.1.2 Cyclic loading tests

To provide a more detailed understanding of the above deformation, sequential load–unloading cycles were performed on samples with polished tensile and adjacent side face. These materials were loaded to increasing maximum force and between each cycle the tensile and side surfaces were visually inspected. Such a testing procedure enabled us to quantify the surface deformation bands on the tensile surface that formed perpendicular to the longitudinal axis and their extension on the side surface. Typical P–δ curves and associated AE, P–N_Σ curves are shown in Figs 3–6 (a and b) for all the Ce–TZP materials. The location

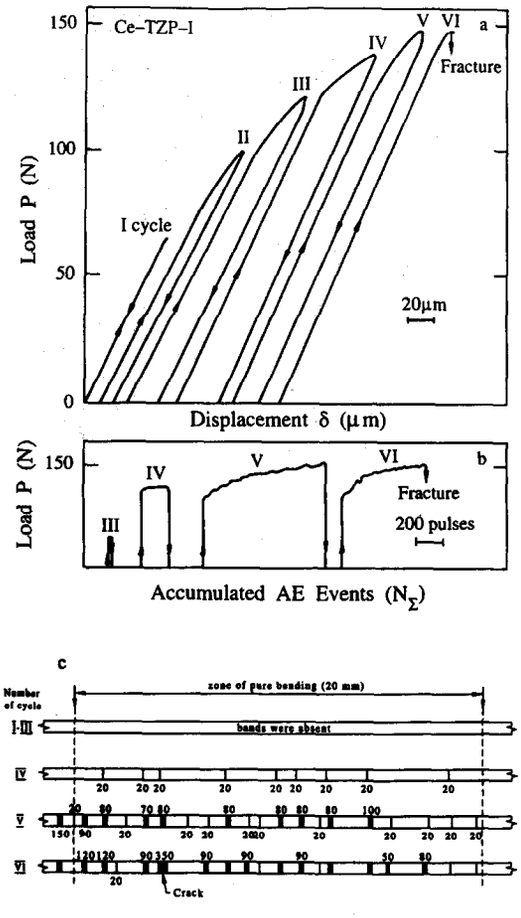

Fig. 3. (a) Cyclic load–displacement data; (b) accumulated AE events; and (c) location and width (in μm) of transformation bands in Ce–TZP-I.

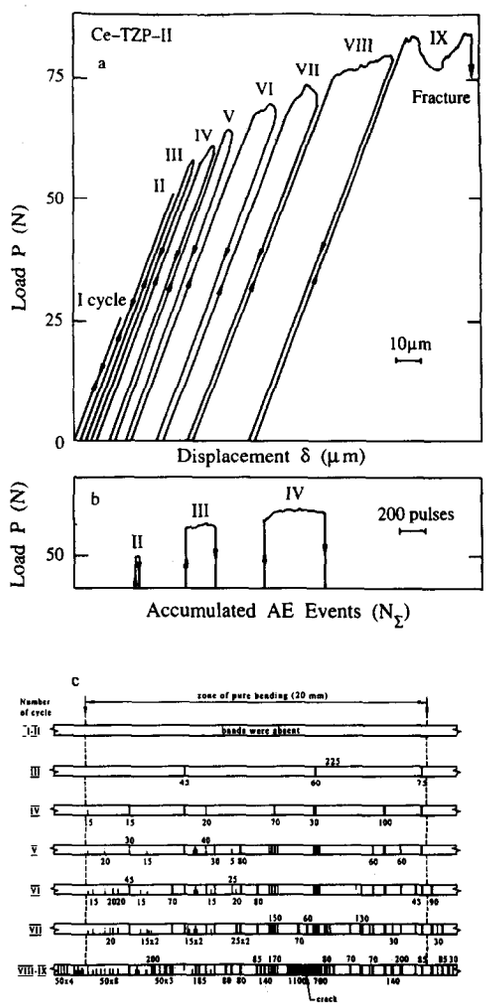

Fig. 4. (a) Cyclic load–displacement data; (b) accumulated AE events; and (c) location and width of transformation bands in Ce–TZP-II.

and size of the transformation bands on the tensile surface are shown in Figs 3–6(c) again for all the Ce–TZP materials. Representative micrographs of the transformation bands on the tensile and side surfaces for samples Ce–TZP-I to -III are shown in Fig. 7. In some instances the transformation band associated with the fracture surface is also visible in the micrograph. Previous examples of this type of deformation for Ce–TZP materials was first shown by Hannink and Swain[3] and reproduced by other authors.[2,4,6]

The present observations enable the following critical aspects of these transformation bands to be made:

(i) Deformation bands appear to initiate randomly and increase in number with increasing strain. They appear to be uniformly distributed within the region of constant stress of the four point flexure specimen. The bands are present only above a critical load (or stress) that for specimens Ce–TZP-II to -IV corresponds to the onset of permanent set or 'plastic' deformation, whereas for material Ce–TZP-I the initial stages of permanent set are not associated with band formation.

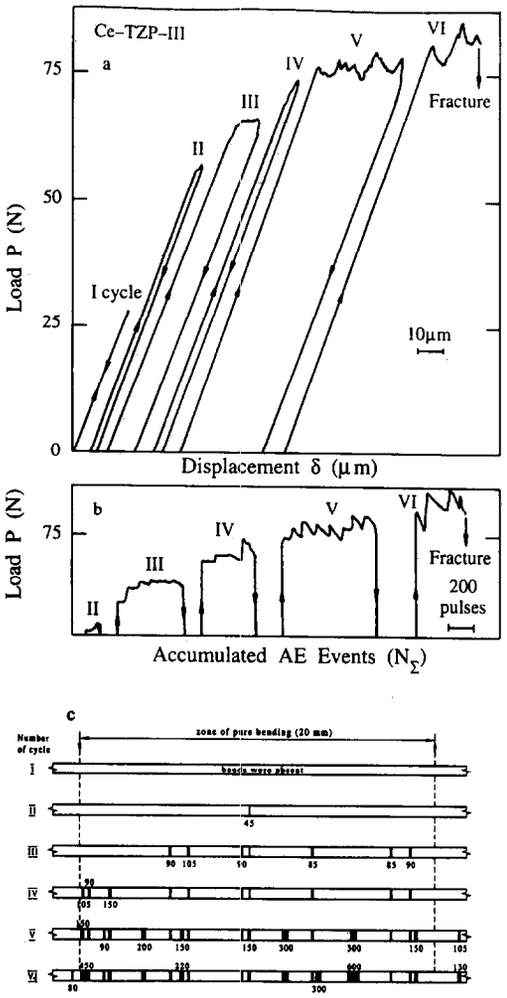

Fig. 5. (a) Cyclic load–displacement data; (b) accumulated AE events; and (c) location and width of transformation bands in Ce–TZP-III.

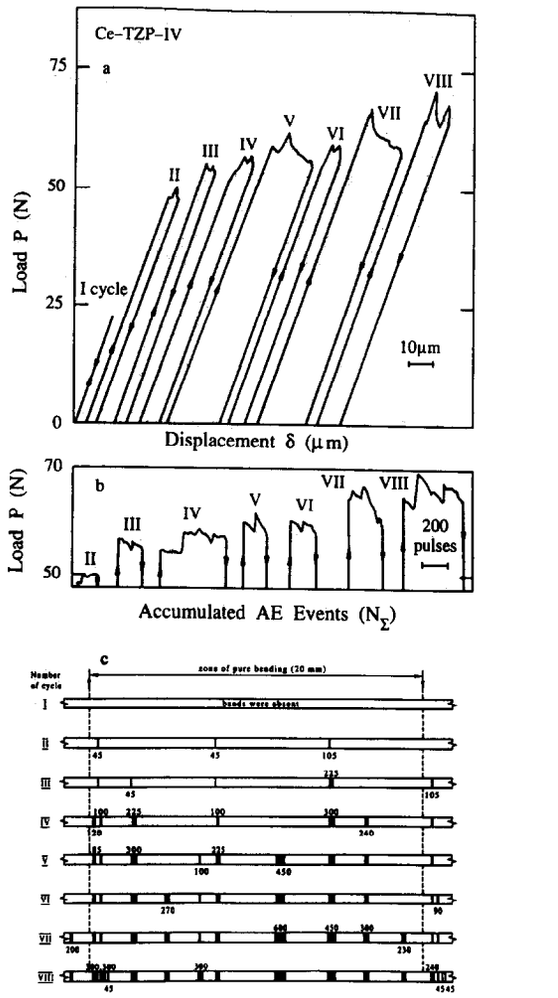

Fig. 6. (a) Cyclic load–displacement data; (b) accumulated AE events; and (c) location and width of transformation bands in Ce–TZP-IV.

(ii) With increasing loading cycles beyond the elastic limit new bands appear and those which were initiated during a previous cycle either increase in width discretely or remain unchanged up to fracture.

(iii) For each cycle the slope of the P–δ curve remains constant upon loading and unloading although the proportionality limit increases with each subsequent cycle. Upon loading to the proportional limit for each cycle no change in the number and size of the transformation bands or AE events is observed.

(iv) The observation of the first AE event coincided with the formation of the first transformation band for all of the Ce–TZP specimens. However, for sample Ce–TZP-I the first detectable AE event occurred after the onset of considerable 'plastic' strain.

(v) For specimens Ce–TZP-III and -IV, that exhibited more pronounced load drops during either monotonic or cyclic loading, a direct relationship between the number of load drops, AE event bursts and number of transformation bands was observed.

(vi) Fracture of the various specimens occurred almost in the centre of one of the widest pre-existing bands and never occurred at a new location.

A more detailed analysis of the deformation bands and their width at the moment of specimen fracture and a histogram plot of the transformation band widths is shown in Fig. 8. This figure reveals major distinctions between the various samples. In particular, the width of the transformation bands increases with specimen grain size. Thus, for example, whilst for the Ce–TZP-I specimen only narrow bands of width $\Delta_i \sim 20$ μm are formed, they are often grouped together in packets of three or four bands, or more at the fracture location. In contrast for specimens Ce–TZP-II to -IV the bands become increasingly thicker and fewer in number. The total number of transformation bands $n_{tr} = \epsilon n_{\Delta}$, observed on the tensile surface of the fractured specimen is also given on the histogram plots.

Analysis of the total width of the bands versus the number of bands formed during the loading

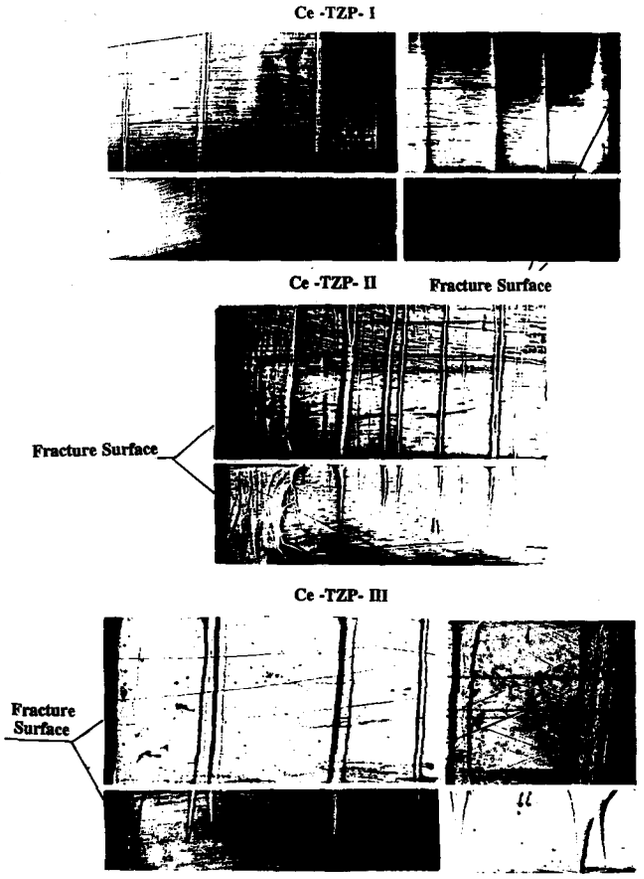

Fig. 7. Typical optical micrographs of the tensile and side faces of various Ce–TZP materials, illustrating the transformation banding.

cycles shows a nonlinear trend and increasing slope with increasing grain size as shown in Fig. 9. This behaviour is most pronounced for samples Ce–TZP-III and -IV, and appears to be related to the magnitude of the load drops with increasing strain during flexure. It is as though the easier initiation sites for transformation band nucleation become exhausted leading to overload conditions

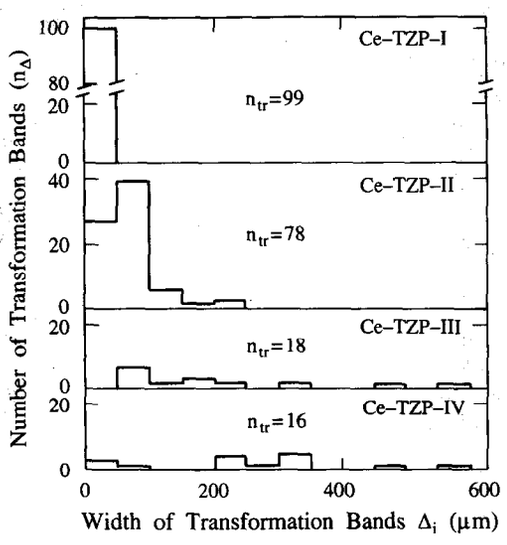

Fig. 8. Histograms of the number (n_Δ) and width (Δ_i) of the transformation bands developed on the tensile surface of the Ce–TZP materials.

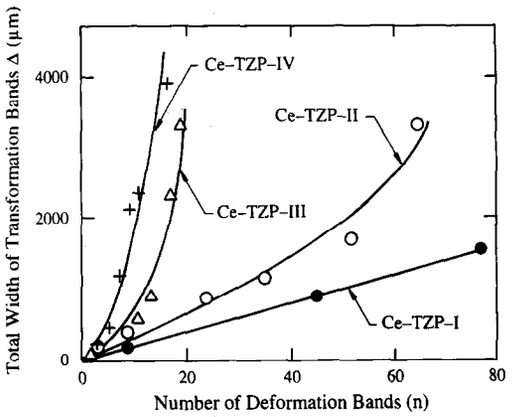

Fig. 9. Relationship between the total transformation band widths Δ versus the number of bands.

for the more difficult sites. This overload instability initiation condition leads to the formation of wider bands.

A more linear relationship may be established between the residual 'plastic' displacement δ_r and the sum of the widths of the transformation bands during each cycle as shown in Fig. 10. The obvious exception to the near universal curve is Ce–TZP-I, which in contrast to that shown in Fig. 9 is very nonlinear. For samples Ce–TZP-II to -IV a linear relationship of the form ($\delta_r = k_i \Delta$) fits the data very well, with the constant k_i tabulated for these materials in Table 3. It is not clear why sample Ce–TZP-I does not show such a linear dependence although it may be due to the presence of some fine scale microcracking as well as transformation that accounts for the significant plastic strain measured. However, one might have expected such microcracking to be associated with a reduction of specimen compliance with each loading cycle. Alternatively, some transformation reversibility upon unloading may occur, but this would be anticipated to have produced some non-linearity during the unloading phase. Perhaps with this sample some ferro-elastic tetragonal grain reorientation

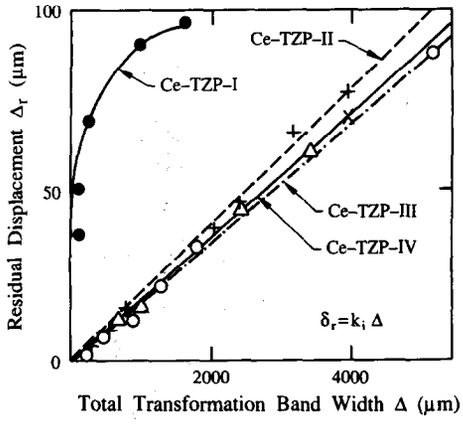

Fig. 10. Relationship between the residual displacement δ_r and the sum of the transformation band widths Δ.

Table 3.

Ceramics	k_1	k_2
Ce–TZP-I	—	25
Ce–TZP-II	0·0193	71
Ce–TZP-III	0·0177	117
Ce–TZP-IV	0·0169	126

as proposed by Virkar and Matsumoto[11] may be occurring during loading which is irreversible upon unloading. If this is the case then it suggests that the fine grained Ce–TZP material initially responds above a critical tensile stress to re-orientation of some tetragonal grains. Upon further loading these or perhaps other sites undergo transformation to monoclinic zirconia. Both of these processes (re-orientation and phase transformation) are associated with residual deformation. The absence of AE events during the initial phase of non-linear response of the Ce–TZP-I material (Fig. 1(a)) is also supportive of this interpretation.

It would be anticipated that because of the observed relationship between δ_r and the sum of the deformation bands Δ, a similar correlation should exist with the inelastic strain ϵ_r of the flexure specimen. For this purpose consider the point Δ = 4000 μm and δ_r = 70 μm (marked as a cross in Fig. 10), which may be thought of as the averaged value for specimens -II to -IV. Then using the simple relationship between strain, ϵ, to the flexure of a beam of height h and inner span length L (20 mm) namely

$$\epsilon = \frac{4h}{L^2}\,\delta\,,$$

this simple hypothesis may be confirmed. Upon substituting for h and δ_r(2·8 mm and 70 μm, respectively), $\epsilon_r = 1{\cdot}7 \times 10^{-3}$. Whereas taking into account that during the phase transformation of tetragonal to monoclinic zirconium oxide there is a volume dilation, ΔV ~4%, which is a linear strain of only ~1/3 (ΔV), that is 1·3%. Therefore, the anticipated 'plastic' strain associated with the total transformation band width is ~4000 μm × $1{\cdot}3 \times 10^{-2} \simeq 52$ μm and, therefore, its value is

$$\epsilon_i^{\Delta} \simeq \frac{\Delta l}{l} = \frac{52 \times 10^{-6}}{20 \times 10^{-3}} = 2{\cdot}6 \times 10^{-3}.$$

The difference between the predicted ϵ_i^{Δ} and measured strain ϵ_r may be accounted for if not all the tetragonal grains within the band are transformed to monoclinic. The present calculation suggests that less than 65% is transformed which is in reasonable agreement with micro-Raman measurements of the phase content of similar transformation bands in a 12 mol% Ce–TZP material by Becher and Swain.[7]

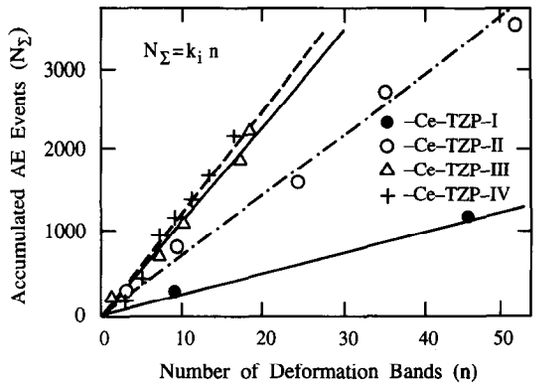

Fig. 11. Correlation between the total AE event count and the number of transformation bands.

Another interesting aspect of the present observations is the comparison of the number of AE pulses N_Σ obtained for a given number of loading cycles with the number of transformation bands, n (Fig. 11). This figure shows an excellent linear relationship for all the Ce–TZP materials with the slope increasing from sample I to IV. That is, this data may be represented by the simple expression $N_\Sigma = k_2 n$ where k_2 is given in Table 3 for all samples. Considering that AE events are associated with the appearance of deformation bands, one may assume that individual AE events are the result of burst like nucleation of such a band.

It is tempting to try to interrelate the observed strain hardening, increasing width of the bands, and the increasing magnitude of the load drops and AE events during the present experiments. Unlike metallic materials the strain hardening does not appear to be related to dislocation (or band) interaction or pile-up processes. Rather it is as though there is a distribution of defects within the materials that provide stress concentration sites from which the transformation bands are nucleated. Thus within the uniform tensile stress zone the initiation load or stress generates a critical tensile strain energy density at the largest defect site (flaw, pore or inclusion). When this local energy density exceeds a critical value it is released as a transformation band which lowers the total strain energy of the beam. As there is likely to be a distribution of such defect sizes within the beam the load must be increased to initiate a transformation band from the next most potent defect site upon the exhaustion of the previous largest defect. However, the increased total strain energy of the beam has the potential to form a wider band of transformation in the otherwise near homogeneous material. This process will continue until a pre-existing or newly initiated band results in the specimen fracture. A more detailed discussion of the fracture of this material is given in the accompanying paper.[12]

4 Conclusions

The present observations have shown the influence of grain size on the deformation behaviour of these 9 mol% Ce–TZP materials. It has been established, as previously shown by Becher and Swain,[7] that the onset of plastic deformation or ease of stress induced phase transformation is grain size dependent.

This study has established a relationship between the grain size and the width of the transformed bands generated on the tensile surface. It has also been shown that for the coarser grained Ce–TZP-II to -IV materials there is a linear relationship between the sum of the width of the transformation bands and the residual plastic strain ϵ_t. A simple analysis of this situation indicated that the accumulated strain was less than anticipated assuming all the tetragonal grains within the band transformed to monoclinic zirconia. The results could be rationalized if only 65% of the grains transformed which is in good agreement with Raman microprobe measurements of such bands by Becher and Swain.[7] It is suggested that a ferro-elastic grain re-orientation may be responsible for the observance of non-linear behaviour of the fine grained Ce–TZP-I material in the absence of transformation bands. Acoustic emission data showed a linear relationship between the number of bands and total AE events.

Acknowledgements

The authors wish to thank Dr T. S. Liu and Dr Grathwohl for the provision of the samples used in these tests. Collaboration was made possible by a grant from the Australian Department of Industry, Technology and Regional Development under the Bilateral Science Program.

References

1. Tsukuma, K. & Shimada, M., Strength, Fracture Toughness and Vickers hardness of CeO_2-stabilised ZrO_2, polycrystals (Ce–TZP). *J. Mater. Sci.*, **20** (1985) 1178.
2. Grathwohl, G. & Liu, T. S., Crack Resistance and Fatigue of Transforming Ceramics: II. CeO_2-stabilised Tetragonal ZrO_2. *J. Am. Ceram. Soc.*, **74** (1991) 3028.
3. Hannink, R. H. J. & Swain, M. V., Metastability of the Martensitic Transformation in a 12 mol% Ceria–Zirconia Alloy: I. Deformation and Fracture Observation. *J. Am. Ceram. Soc.*, **72** (1989) 90–8.
4. Reyes-Morel, P. E. & Chen, I.-W., Deformation Plasticity of CeO_2 Stabilised Tetragonal Zirconia Polycrystals: I. Stress Assistance and Autocatalysis. *J. Am. Ceram. Soc.*, **71** (1988) 343.
5. Swain, M. V. & Hannink, R. H. J., Metastability of the Martensitic Transformation in a 12mol% Ce–TZP Alloy: II. Grinding Studies. *J. Am. Ceram. Soc.*, **72** (1989).
6. Yu, C.-S. & Shetty, D. K., Transformation Zone Shape, Size and Crack Growth Resistance (*R*-Curve) Behaviour of Ceria Partially Stabilised Zirconia Polycrystals. *J. Am. Ceram. Soc.*, **72** (1989) 921.
7. Becher, P. F. & Swain, M. V., Grain Size Dependent Transformation Behaviour in Polyerystalline Tetragonal Zirconia. *J. Am. Ceram Soc.*, **75** (1992) 493.
8. Drozdov, A. V., Galenko, V. O., Gogotsi, G. A., Fasenko, F. A. & Swain, M. V., Acoustic Emission During Micro and Macrocrack growth in Mg–PSZ. *J. Am. Ceram. Soc.*, **74** (1991) 1922–7.
9. Gogotsi, G. A., Drozdov, A. V., Zavada, V. P. & Swain, M. V., Comparison of the Mechanical Behaviour of Zirconia Partically Stabilised with Yttria and Magnesia. *J. Aust. Ceram. Soc.*, **27** (1991) 37.
10. Gogotsi, G. A., In *Advanced Ceramics.* eds C. Ganguly, S. K. Roy & P. R. Roy. Trans. Tech. Publ., USA (1991) p. 411.
11. Gogotsi, G. A., Deformational Behaviour of Ceramics. *J. Eur. Ceram. Soc.*, **7** (1991) 87.
12. Virkar, A. V. & Matsumoto, R. L. K., Ferroelastic Domain Switching as a Toughening Mechanism in Tetragonal Zirconia. *J. Am. Ceram. Soc.*, **69** (1986) C224.
13. Gogotsi, G. A., Zavada, V. P. & Swain, M. V., Mechanical Property Characterisation of a 9% Ce–TZP Ceramic Material: II. Fracture Toughness. *J. Eur. Ceram. Soc.*, in press.